Bioorganic & Medicinal Chemistry 17 (2009) 6803–6810

Contents lists available at ScienceDirect

Bioorganic & Medicinal Chemistry

journal homepage: www.elsevier.com/locate/bmc

Recognition of CG interrupting site by W-shaped nucleoside analogs (WNA) having the pyrazole ring in an anti-parallel triplex DNA

Yosuke Taniguchi [a,b], Yuko Uchida [a], Tomoko Takaki [a], Eriko Aoki [a,b], Shigeki Sasaki [a,b,*]

[a] Graduate School of Pharmaceutical Sciences, Kyushu University, 3-1-1 Maidashi, Higashi-ku, Fukuoka 812-8582, Japan
[b] CREST, Japan Science and Technology Agency, Center Building, 4-1-8 Honcho, Kawaguchi, Saitama 332-0012, Japan

ARTICLE INFO

Article history:
Received 13 July 2009
Revised 18 August 2009
Accepted 19 August 2009
Available online 22 August 2009

Keywords:
W-shaped nucleoside analog (WNA)
Anti-parallel triplex
Antigene
5-Membered heterocycle
Nucleoside analog
Triplex DNA
CG interrupting site
Synthesis
Evaluation

ABSTRACT

We have previously developed W-shaped nucleoside analogs (WNA) for recognition of TA and CG interrupting sites, which are the intrinsic limitation for the formation of a stable triplex DNA by the natural triplex-forming oligonucleotide (TFO). However, the stabilization effect of WNA is dependent on the neighboring nucleobases at both sides of the WNA analogs within the TFO. Considering that the base is located at the hindered site constructed of three bases of the target duplex and the TFO, it was expected that replacement of the pyrimidine base of the WNA analog with a smaller pyrazole ring might avoid steric repulsion to produce a greater stability for the triplex. In this study, the new WNA analogs bearing the pyrazole ring, 3-aminopyrazole (AP), and 4-methyl-3-pyrazole-5-on (MP) were synthesized, incorporated into the TFOs, then their stabilizing effects on the triplexes were evaluated. A remarkable success was illustrated by the fact that the TFO containing WNA-βAP in the 3′G-WNA-G-5′ sequence formed a stable triplex with selectivity to the CG interrupting site where the previous WNA-βC did not induce the triplex formation.

1. Introduction

Triplex-forming oligonucleotides (TFOs) associate with the major groove of a duplex DNA and has attracted interest as potential tools for genomic therapy, research, and technology.[1–7] In the anti-parallel triplex, the most stable triplex DNA is formed by the interaction between the purine-rich TFO and homopurine/homopyrimidine regions of the duplex DNA in a sequence specific manner (dG/GC, dA/AT).[8] Therefore, the stable triplex DNA is hampered by one pyrimidine base insertion in the homopurine strand (TA and CG pairs are called interrupting sites). Despite numerous studies, this problem has not yet been fully solved.[9–13]

We previously showed that W-shaped nucleoside analogs (WNAs), WNA-βT and WNA-βC, recognized the TA and CG interrupting site with a high selectivity, respectively (Fig. 1).[14–16] Subsequently, it turned out that the recognition abilities of the WNA analogs were affected by the neighboring nucleobases on the both sides of the WNA. As the origin of a neighboring bases effect on triplex stability, especially in the case of triplexes containing non-natural base analogs, is not well understood,[11,12] we initiated a systematic investigation using a variety of WNA analogs with a small structural change to overcome this problem. A number of modified WNA-βT derivatives were constructed with the *o*-, *m*-, *p*-bromo-, *p*-cyano, *p*-amino substituted benzene, or 3-pyridine unit. The individual WNA derivative was determined to recognize the TA interrupting site of each sequence, for example, the original WNA-βT in the 3′-AZG-5′ and the 3′-GZG-5′ TFO, *o*-bromo-WNA-βT

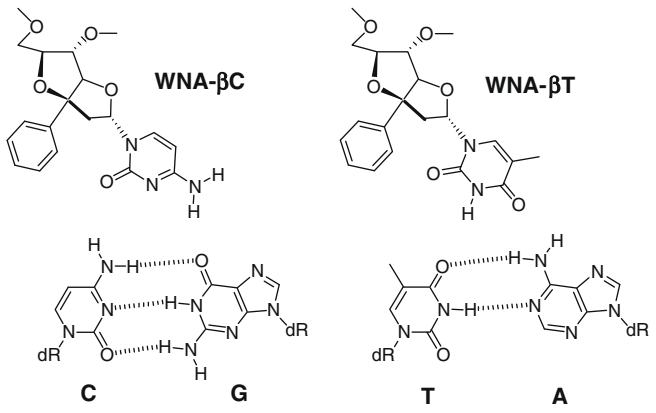

Figure 1. Speculated recognition structure of WNA-βC/CG and WNA-βT/TA combinations. WNA (W-shaped nucleoside analogs).

* Corresponding author. Tel./fax: +81 92 642 6651.
E-mail address: sasaki@phar.kyushu-u.ac.jp (S. Sasaki).

0968-0896/$ - see front matter © 2009 Elsevier Ltd. All rights reserved.
doi:10.1016/j.bmc.2009.08.040

in the 3′-AZA-5′ TFO, *m*-bromo-WNA-βT and *p*-cyano-WNA-βT in the 3′-GZA-5′ TFO (Z = WNA analog) have been shown to be suitable for stabilization of the triplex having the corresponding TA interrupting site.[17–19] Thus, the combined use of the aromatic-modified WNA analogs has provided a partial solution of the sequence-dependency problem of the WNA-βT analog. Nevertheless, a general solution for the TA and CG interrupting site of the triplex is still a challenging theme. In addition to the important role of the benzene part, the effects of the recognition unit of the WNA analog are somewhat complicated as shown by the facts that the order of the stabilization effect on the triplexes is WNA-H lacking the recognition base with non-selectivity > WNA-βT with high selectivity > WNA-7βG having N^7-guanine base with a low stabilization effect.[15] These results have indicated that the size of the recognition base significantly affects the triplex stability. These considerations encouraged us to study replacement of the pyrimidine base of the WNA analog with a smaller pyrazole ring to avoid steric repulsion and to enhance hydrogen bond formation. In this paper, we describe in detail the synthesis and evaluation of the triplex forming ability of the new WNA analogs, WNA-βAP and -αAP containing 3-aminopyrazole and WNA-βMP and -αMP containing 4-methyl-3-pyrazole-5-on, whose hydrogen-bonding motifs are similar to cytosine and thymine, respectively (Fig. 2).

2. Results and discussion

Synthesis of the phosphoramidite derivatives of the WNA analog with the 3-aminopyrazole unit (WNA-AP) was accomplished as shown in Scheme 1. The amino group of 3-aminopyrazole (AP) was protected by *N,N*-dimethylformamidedimethylacetal to give **1** in good yield.[20] The protected aminopyrazole (**1**) was coupled with the bicyclic sugar intermediate **2**[14,15] to produce regioselectively the N^1-glycosidated products **3a** (20%) and **3b** (41%) after separation by silica gel column chromatography, whose stereochemistry was determined by their ^{1}H-COSY and -NOESY spectra (Fig. 3). Each isomer was subjected to deprotection of the TBDPS and the acetyl groups to afford the corresponding diol compounds **4a** (93%) and **4b** (97%). These diol compounds were converted to the corresponding phosphoramidite precursor by the conventional method (WNA-αAP; **5a** in 60%, WNA-βAP; **5b** in 66%). The TFOs (**TFO 1**, **2**, **3**, and **4**) containing the WNA-AP derivative were obtained in good yield using an automated DNA synthesizer. **TFO1(βAP)** represents the **TFO1** containing WNA-βAP at position Z in the sequence of 3′-AZG-5′. Cleavage of the synthesized TFO from the CPG column and the deprotection of the aminopyrazole unit were done in a solution of 28% NH_4OH at 55 °C for 5 h. After purification by reversed-phase HPLC, the synthesized TFOs were identified by MALDI-TOF MS measurements.

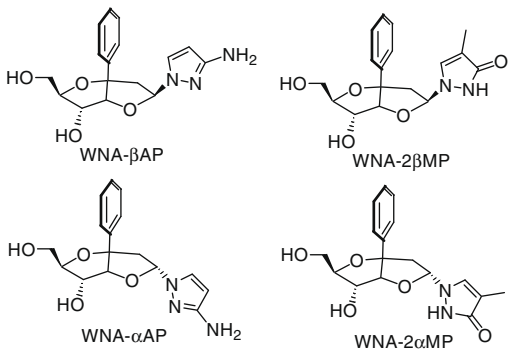

Figure 2. Design of new WNA analogs, WNA-AP and WNA-2MP (AP: 3-aminopyrazole, MP: 4-methyl-3-pyrazole-5-on).

On the other hand, the WNA analogs with the 4-methyl-3-pyrazole-5-on unit (WNA-MP) were synthesized as shown in Scheme 2. 4-Methyl-3-pyrazole-5-on (MP)[21] was treated with benzoyl chloride to afford **6** in good yield. As the benzoyl group of **6** migrated to the other position, we used MP-Bz as the mixture of regioisomers for the following coupling reaction without separation. The coupling of **6** with the bicyclic sugar intermediate **2** gave four isomers **7a** (13%), **7b** (10%), **8a** (20%), and **8b** (11%). Fortunately, these isomers could be completely separated by silica gel column chromatography, and the regiochemistry and the stereochemistry of each isomer were determined by its ^{1}H-COSY and NOESY spectra after removal of the TBDPS, acetyl and benzoyl groups; WNA-2αMP (**9a**) in 78%, WNA-2βMP (**9b**) in 72%, WNA-1αMP (**10a**) in 42%, WNA-1βMP **10b** in 44% (Fig. 4). The coupling position of the 4-methyl-3-pyrazole-5-on unit (MP) was unambiguously determined by the NOE cross peaks with 3-H; the 2-coupled products (**9a** and **9b**) did not produce cross peaks with the protons of the sugar part, whereas the 1-coupled products (**10a** and **10b**) showed cross peaks with the protons of the sugar part as illustrated in Figure 4. At the same time, the stereochemistry of each isomer was determined. The desired diol compounds (**9a** and **9b**) were converted to the corresponding phosphoramidite precursor; WNA-2αMP (**11a**) in 51% yield, WNA-2βMP (**11b**) in 39% yield (Scheme 3). Unfortunately, the diol compounds (**10b** and **10a**) led to multiple compounds using the same protection process. Therefore, we adopted WNA-2βMP and WNA-2αMP for incorporation into the TFO. The TFOs (**TFO 1**, **2**, **3**, and **4**) having the WNA-2α or βMP derivative were obtained in good yields using an automated DNA synthesizer. The cleavage of the synthesized TFO from the CPG resin was performed in a 28% NH_4OH solution at room temperature to prevent the removal of the pyrazole recognition base. After separation by HPLC, the purity and structure of the TFOs were confirmed by MALDI-TOF MS measurements.

The triplex forming abilities of the TFOs containing the WNA analogs were evaluated by the gel-shift assay using the ^{32}P-labeled TFO as a tracer. The intensities of the radioactive bands were measured from which the association constants (K_s values) of the triplex formations were calculated as previously described.[15] The examples of the electrophoresis of TFO containing WNA-βAP in the sequence of 3′-dG and 5′-dG (**TFO2(βAP)**) are shown in Figure 5. The high mobility bands showed the single stranded TFO, on the other hand, the low mobility bands showed the triplex DNA. The triplex bands were observed at low TFO concentrations in Figure 5A, clearly indicating that **TFO2(βAP)** stabilized the triplex DNA having the CG interrupting site with a high selectivity. The association constant (K_s value) of all the TFOs are summarized in Figure 6. We previously reported that **TFO1(βC)** having WNA-βC in the TFO sequence of 3′-AZG-5′ could stabilize the CG interrupting site (Fig. 6A, green bars). **TFO1(βAP)** incorporating the aminopyrazole unit with the β-stereochemistry formed a stable triplex with the GC pair at the complementary site (Fig. 6A, blue bars). **TFO1(αAP)**, **TFO1(2βMP),** and **TFO1(2αAP)** indicated relatively higher stabilization effects for the CG pair, although these stabilities and selectivities were insufficient (Fig. 6A, pink and orange bars). Based on these results, the recognition behavior of the pyrazole ring were not clear in the sequence of TFO1 (3′AZG). Remarkable results were obtained with **TFO2** in the sequence of 3′-GZG-5′ (Fig. 6B), where the original WNA-βC was also not able to form stable triplexes (Fig. 6B, green bars). **TFO2(βAP)** exhibited a high affinity for the target DNA with the CG interrupting site (Fig. 6B, blue bars). It is noteworthy that the CG recognition affinity of WNA-βAP is higher than the natural dG/GC triplet. In this TFO sequence, a shortcoming of the original WNA-βC was overcome with WNA-βAP. Unfortunately, **TFO2** with other WNA analogs (**αAP**, **2βMP**, **2αMP**) did not show interesting stabilizing effects (Fig. 6B). The results of **TFO3** in the sequence of 3′-GZA-5′ are summarized in Figure 6C.

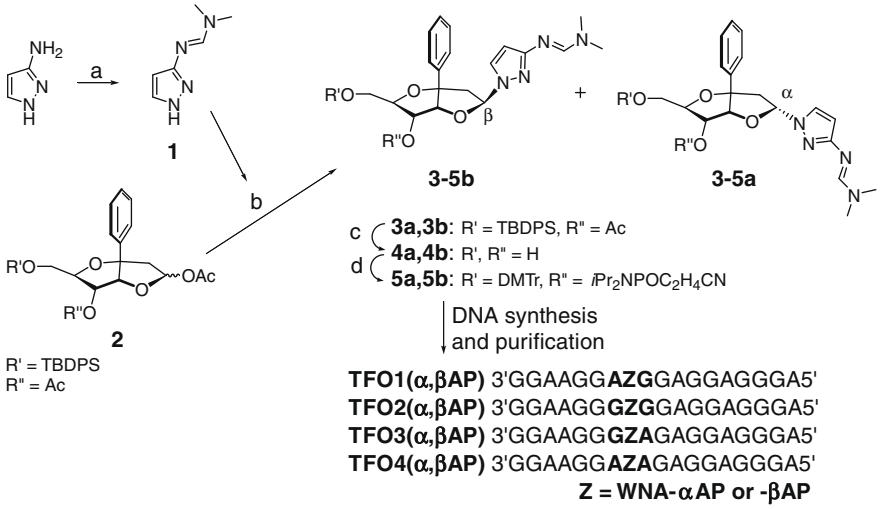

Scheme 1. Reagents and conditions: (a) *N,N*-dimethylformamidedimethylacetal, 100 °C, (92%); (b) **1**, BSA, TMSOTf, CH_3CN, rt (**3b**: WNA-βAP; 41%, **3a**: WNA-αAP; 20%); (e) (1) TBAF, THF, rt, (2) 0.2 M NaOHaq, MeOH, THF, 0 °C (**4b**: WNA-βAP; 97%, **4b**: WNA-αAP; 93% for two steps); (f) (1) DMTrCl, pyridine, (2) $iPr_2NP(Cl)OCH_2CH_2CN$, DIPEA, CH_2Cl_2, 0 °C (**5b**: WNA-βAP; 66%, **5a**: WNA-αAP; 60% in two steps).

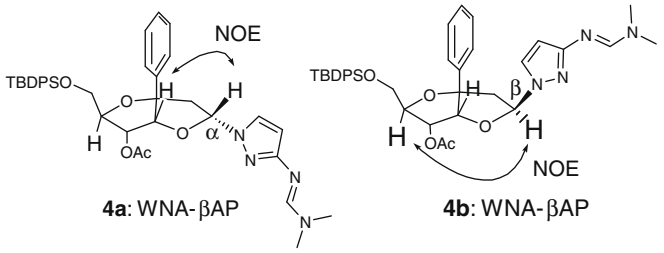

Figure 3. NOESY result for the determination of the stereochemistry at the anomeric position of the WNA-AP derivatives.

In contrast to the original WNA-βC that did not produce any triplex stability in the **TFO3** sequence, interesting binding profiles were observed for all the new WNA analogs; WNA-βAP for the AT site, WNA-αAP for all four base pairs, WNA-βMP for the AT and GC pairs, and WNA-2αMP for the GC pair. In particular, the triplex stability formed with WNA-MP was similar to those formed with the natural dG/GC triplet (Fig. 6C, yellow bars vs pink and orange bars). As the WNA analog lacking a heterocyclic unit in the **TFO3** sequence showed no stabilizing effect to any base pairs,[18] it is apparent that the pyrazole recognition base has a benefit for improving of the triplex stability with the WNA analogs. In the case of **TFO4** in the sequence of 3′-AZA-5′ where **TFO4(βC)** did not form the triplex DNA at any target base pair, **TFO4(βAP)** formed triplexes for the GC and AT pairs in the target duplexes, suggesting that the small recognition base may have a structural benefit for recognition in this sequence (Fig. 6D, blue bars). The **TFO4** sequences having other WNAs (**αAP**, **2βMP**, **2αMP**) have a similar tendency for triplex stability although their complex stability constants were not sufficient (Fig. 6D).

3. Conclusion

In this study, by expecting that replacement of the pyrimidine base of the WNA analog with a smaller pyrazole ring might avoid steric repulsion with the base pair of the target duplex to produce a greater stability for the triplex, the new WNA analogs with 3-aminopyrazole or 4-methyl-3-pyrazole-5-on were designed, incorporated into the TFOs, and evaluated for their stabilizing effect of the triplexes. A remarkable success has been illustrated by the formation of a stable triplex with WNA-βAP in the TFO sequence of 3′-GZG-5′ toward the target duplex having the CG interrupting site. From the fact that the smaller pyrazole ring was useful for improvement of the triplex formation, this study has provided use-

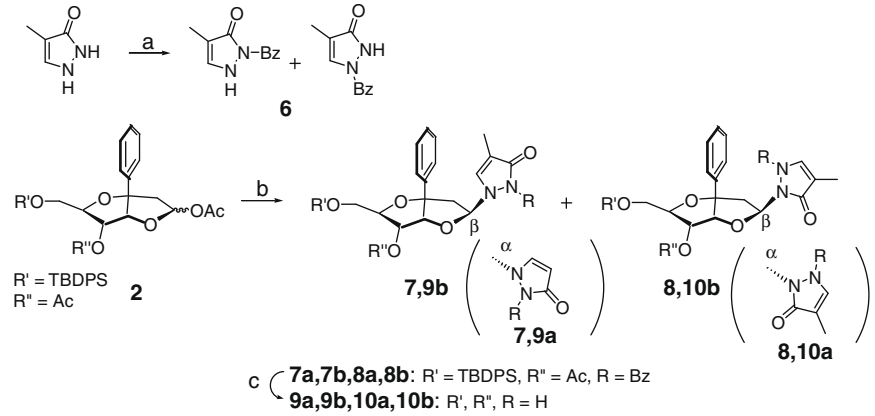

Scheme 2. Reagents and conditions: (a) BzCl, pyridine, (86%); (b) **6**, BSA, TMSOTf, CH_3CN, rt (**7b**: WNA-2βMP; 10%, **7a**: WNA-2αMP; 13%, **8b**: WNA-1βMP; 11%, **8a**: WNA-1αMP; 20%); (c) (1) TBAF, THF, rt, (2) 0.2 M NaOHaq, MeOH, THF, 0 °C (**9b**: WNA-2βMP; 72%, **9a**: WNA-2αMP; 78%, **10b**: WNA-1βMP; 44%, **10a**: WNA-1αMP; 42% in two steps).

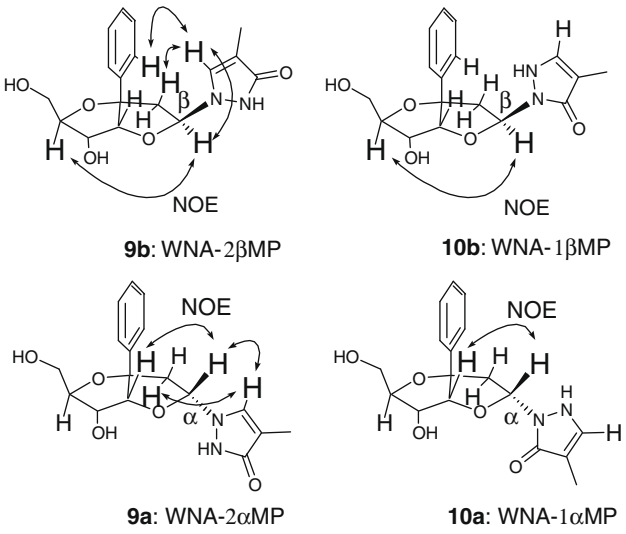

Figure 4. NOESY result for the determination of the stereochemistry and regiochemistry of WNA-MP.

ful information for further optimization of the WNA analog for triplex stabilization.

4. Experiments

4.1. General

The ^{1}H NMR (400 MHz), ^{13}C NMR (125 MHz) and HH-COSY, NOESY spectra were recorded using Varian UNITY-400 and INOVA-500 spectrometers. The ^{31}P NMR (161 MHz) spectrum was recorded using 10% phosphoric acid in D_2O for the internal standard at 0 ppm. The IR spectra were obtained using a Perkin Elmer FTIR-SpectrumOne. The high-resolution mass spectra were recorded by an Applied Biosystems Mariner System 5299 spectrometer using nicotinic acid, bradykinin and neurotensin as the internal standard. The MALDI-TOF/MS spectra were recorded by a Bruker Microflex using 3-hydroxypicolinic acid matrix.

4.1.1. N^3-Dimethylaminomethylidine-3-aminopyrazole (1)

N,N-Dimethylformamidedimethylacetal (0.53 mL, 4.14 mmol) was added to a solution of 3-aminopyrazole (207 mg, 2.44 mmol) in methanol (8.0 mL). The reaction mixture was refluxed at 100 °C for 1 h, and then the solvent was evaporated under reduced pressure. The residue was treated with hexane and the precipitates were collected, which were recrystallized from ether/ethanol = 9:1 to give a pale green solid (312 mg, 2.26 mmol, 92%). ^{1}H NMR (400 MHz, $CDCl_3$): δ 7.85 (1H, s), 7.37 (1H, d, J = 2.0 Hz), 5.82 (1H, d, J = 2.0 Hz), 3.01 (6H, s). ^{13}C NMR (125 MHz, $CDCl_3$): 155.0, 135.8, 91.8, 40.5, 34.7. FTIR (neat): 3151, 1645, 1541, 1403 cm^{-1}. HRMS (ESI) m/z: calc for $C_6H_{11}N_4$ $(M+H)^+$ 139.0978, found 139.0978.

4.1.2. N^1- and N^2-Benzoyl-4-methyl-3-pyrazolin-5-one (6)

Benzoyl chloride (0.3 mL, 2.56 mmol) was added to a solution of 4-methyl-3-pyrazolin-5-one (251 mg, 2.56 mmol) in pyridine (15 mL). After stirring for 2.5 h, the reaction was quenched by a 10% aqueous HCl solution and extracted with EtOAc. The organic layer was washed with water and an aqueous saturated NaCl solution, dried over Na_2SO_4, and evaporated. The residue was purified by flash silica gel column chromatography ($CHCl_3$/MeOH = 10:1) to give a mixture of two regioisomers as a colorless oil (448 mg, 2.21 mmol, 86%). ^{1}H NMR (400 MHz, $CDCl_3$): δ 8.19 (1H, dd, J = 1.22, 8.39 Hz), 7.75 (1H, d, J = 7.02 Hz), 7.62 (0.5H, t, J = 7.63 Hz), 7.60 (0.5H, s), 7.57 (0.5H, t, J = 7.33 Hz), 7.48 (1H, t, J = 7.63 Hz), 7.46 (1H, t, J = 7.33 Hz), 7.33 (0.5H, s), 1.96 (1.5H, s), 1.95 (1.5H, s). ^{13}C NMR (125 MHz, $CDCl_3$): 171.3, 165.6, 164.3, 133.4, 132.3, 131.9, 130.8, 130.1, 129.6, 128.4, 128.3, 110.7, 7.0. FTIR (neat): 3205, 2925, 1743, 1697, 1623, 1537, 1261 cm^{-1}. HRMS (ESI) m/z: calcd for $C_{11}H_{11}N_2O_2$ $(M+H)^+$ 203.0815, found 203.0841.

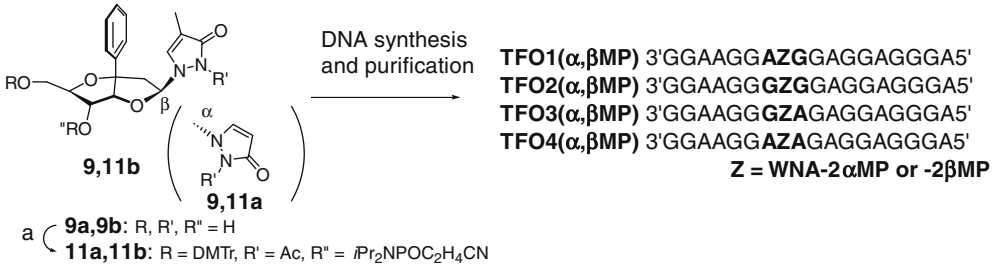

Scheme 3. Reagents and conditions: (a) (1) DMTrCl, pyridine, (2) AcO_2, pyridine, (3) $(iPr_2N)_2POCH_2CH_2CN$, DIPEA, CH_2Cl_2, 0 °C (**11b**: WNA-2βMP; 39%, **11a**: WNA-2αMP; 51% in three steps).

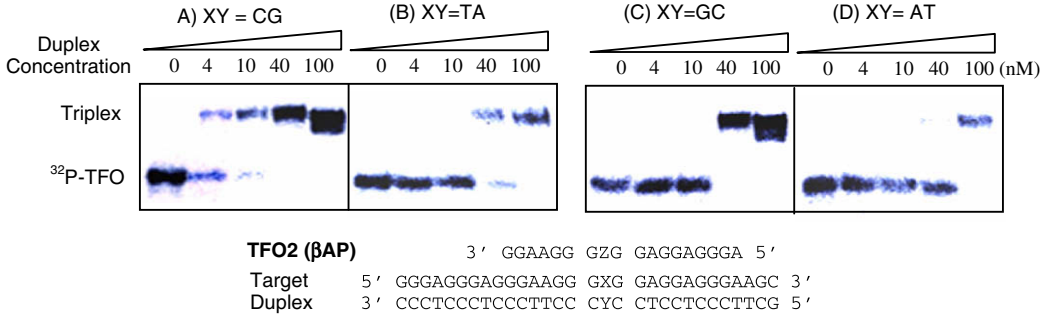

Figure 5. Gel-shift assay for determination of triplex formation of the **TFO2** (**βAP**) containing WNA-βAP in the sequence of 3′- and 5′-dG. The triplex formation was done for 12 h at 22 °C in a buffer containing 20 mM Tris–HCl, 5 mM $MgCl_2$, 2.5 mM spermidine and 10% sucrose at pH 7.5. Electrophoresis was done at 10 °C using 20% non-denatured polyacrylamide gel. Ten nM TFO containing the ^{32}P-labeled one as the tracer was used. The concentration of the duplex was increased; 0, 4, 10, 40, 100 nM.

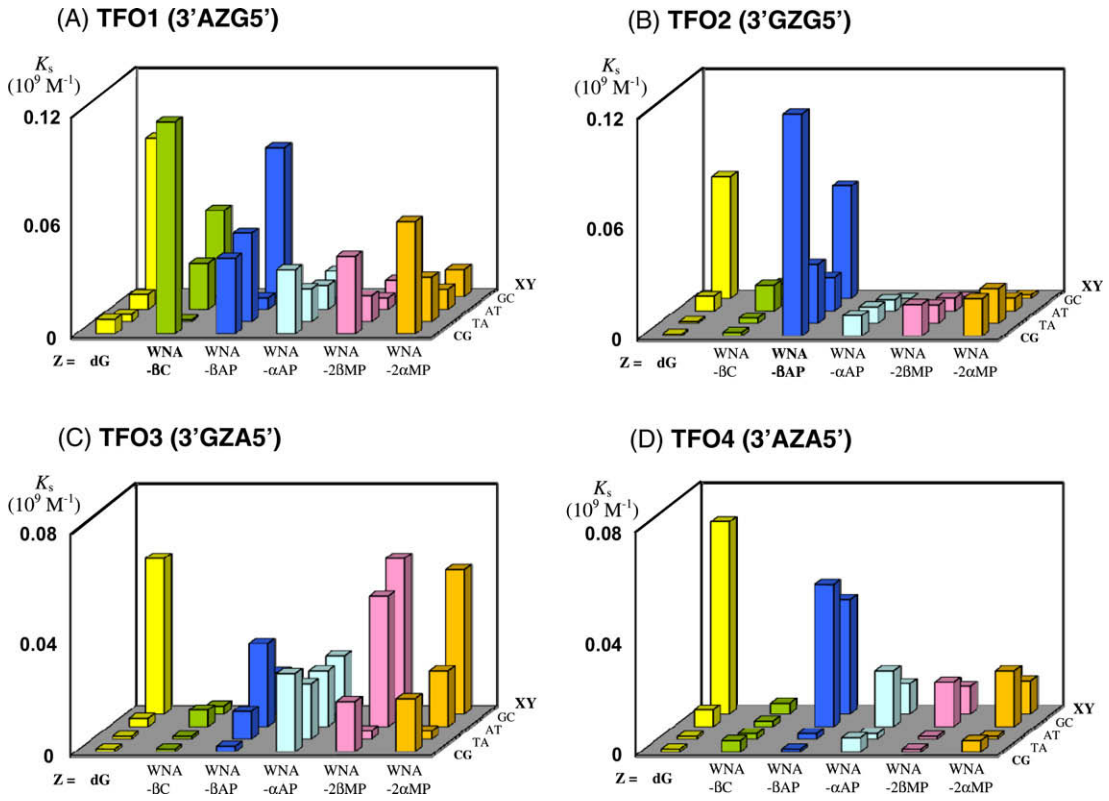

Figure 6. Bar graphs of the association constants (K_s) of the TFOs. These values were calculated from the result of the gel-shift assay the conditions of which were described in Figure 5. K_s = [Triplex]/[ssTFO][Duplex]. (A) **TFO1**; 3′AZG5′, (B) **TFO2**; 3′GZG5′, (C) **TFO3**; 3′GZA5′ and (D) **TFO4**; 3′AZA5′, Z = WNA analogues or dG.

4.2. General procedure for glycosidation reaction

N,O-Bis(trimethylsilyl)acetamide (2.0 equiv) was added to a suspension of the protected pyrazole **1** or **6** (1.0 equiv) in CH_3CN. A solution of TMSOTf (1.0 equiv) and **2** (0.7 equiv) in CH_3CN was added to the above mixture. After stirring for 3 h, the reaction mixture was quenched with an aqueous saturated $NaHCO_3$ solution, and extracted with EtOAc. The organic layer was washed with water and brine, dried over Na_2SO_4, and evaporated. The isomers were separated by flash silica gel column chromatography (hexane/$CHCl_3$/acetone = 2:2:1 to 1:1:1) to give each isomer.

4.2.1. (1′*S*,3′*R*,4′*R*,5′*R*,7′*R*)-*N*^{3}-Dimethylaminomethylidine-1-{4′-acetoxy-1′-phenyl-3′-(*t*-butyldiphenylsilyloxymethyl)-2′,6′-dioxabicyclo[3.3.0]oct-7′-yl}-3-aminopyrazole (3a)

(WNA-αAP) ^{1}H NMR (400 MHz, $CDCl_3$): δ 7.71–7.29 (17H, m), 6.59 (1H, t, J = 7.6 Hz), 5.67 (1H, d, J = 1.8 Hz), 5.09 (1H, dd, J = 4.6, 9.3 Hz), 4.68 (1H, dt, J = 9.2 Hz), 4.66 (1H, d, J = 4.3 Hz), 4.15 (1H, dd, J = 2.4, 11.6 Hz), 3.74 (1H, dd, J = 2.4, 11.9 Hz), 3.53 (1H, dd, J = 7.6, 14.3 Hz), 3.03 (6H, s), 2.83 (1H, dd, J = 7.3, 14.3 Hz), 1.92 (3H, s), 1.03 (9H, s). ^{13}C NMR (125 MHz, $CDCl_3$): 170.2, 154.8, 143.1, 139.9, 135.6, 133.3, 133.2, 129.6, 128.3, 127.7, 127.6, 127.2, 125.3, 91.9, 86.2, 85.9, 78.6, 71.8, 61.8, 46.5, 26.8, 20.7, 19.2. FTIR (neat): 1743, 1635, 1534, 1239 cm^{-1}. HRMS (ESI) *m/z*: calcd for $C_{37}H_{45}N_4O_5Si$ $(M+H)^+$ 653.3154, found 653.3132.

4.2.2. (1′*S*,3′*R*,4′*R*,5′*R*,7′*S*)-*N*^{3}-Dimethylaminomethylidine-1-{4′-acetoxy-1′-phenyl-3′-(*t*-butyldiphenylsilyloxymethyl)-2′,6′-dioxabicyclo[3.3.0]oct-7′-yl}-3-aminopyrazole (3b)

(WNA-βAP) Colorless foam. ^{1}H NMR (400 MHz, $CDCl_3$): δ 7.81–7.26 (17H, m), 6.67 (1H, t, J = 7.0 Hz), 5.68 (1H, s), 5.14 (1H, dd, J = 3.8, 9.3 Hz), 5.04 (1H, d, J = 3.7 Hz), 4.35 (1H, dt, J = 9.2 Hz), 4.02 (1H, dd, J = 2.8, 11.6 Hz), 3.75 (1H, dd, J = 3.7, 11.1 Hz), 3.38 (1H, dd, J = 7.6, 14.2 Hz), 3.02 (6H, s), 2.81 (1H, dd, J = 6.7, 14.2 Hz), 1.96 (3H, s), 1.01 (9H, s). ^{13}C NMR (125 MHz, $CDCl_3$): 169.7, 154.8, 140.8, 140.0, 135.7, 135.6, 133.3, 133.1, 129.7, 129.6, 128.2, 127.7,127.6, 127.3, 125.8, 93.1, 86.4, 86.0, 80.2, 73.0, 63.0, 47.9, 26.8, 20.8, 19.2. FTIR (neat): 1745, 1635, 1533, 1237 cm^{-1}. HRMS (ESI) *m/z*: calcd for $C_{37}H_{45}N_4O_5Si$ $(M+H)^+$ 653.3154, found 653.3126.

4.2.3. (1′*S*,3′*R*,4′*R*,5′*R*,7′*R*)-*N*^{1}-Benzoyl-2-{4′-acetoxy-1′-phenyl-3′-(*t*-butyldiphenylsilyloxymethyl)-2′,6′-dioxabicyclo[3.3.0]oct-7′-yl}-4-methyl-3-pyrazolin-5-one (7a)

(WNA-2αMP) ^{1}H NMR (400 MHz, $CDCl_3$): δ 8.18 (2H, dd, J = 1.2, 7.9 Hz), 7.66–7.24 (19H, m), 6.17 (1H, dd, J = 4.5, 7.6 Hz), 5.00 (1H, dd, J = 4.2, 8.8 Hz), 4.85 (1H, d, J = 3.9 Hz), 4.21 (1H, dt, J = 3.3, 8.8 Hz), 3.98 (1H, dd, J = 3.0, 11.5 Hz), 3.71 (1H, dd, J = 3.9, 11.5 Hz), 3.23 (1H, dd, J = 4.5, 15.1 Hz), 2.94 (1H, dd, J = 7.6, 15.1 Hz), 1.99 (3H, s), 1.94 (3H, s), 0.99 (9H, s). ^{13}C NMR (125 MHz, $CDCl_3$): 170.1, 164.1, 154.2, 141.1, 135.7, 135.6, 133.7, 133.2, 133.1, 131.0, 130.4, 129.7, 127.6, 125.2, 111.5, 108.2, 92.5, 91.9, 87.4, 79.7, 72.5, 62.7, 47.8, 26.8, 20.7, 19.2, 7.6. FTIR (neat): 1745, 1601, 1448 cm^{-1}. HRMS (ESI) *m/z*: calcd for $C_{42}H_{45}N_2O_7Si$ $(M+H)^+$ 717.2991, found 717.3039.

4.2.4. (1′*S*,3′*R*,4′*R*,5′*R*,7′*S*)-*N*^{1}-Benzoyl-2-{4′-acetoxy-1′-phenyl-3′-(*t*-butyldiphenylsilyloxymethyl)-2′,6′-dioxabicyclo[3.3.0]oct-7′-yl}-4-methyl-3-pyrazolin-5-one (7b)

(WNA-2βMP) ^{1}H NMR (400 MHz, $CDCl_3$): δ 8.21 (2H, dd, J = 1.2, 7.0 Hz), 7.68–7.20 (19H, m), 6.09 (1H, t, J = 6.7 Hz), 5.08 (1H, dd, J = 3.9, 9.1 Hz), 4.99 (1H, d, J = 3.9 Hz), 4.28 (1H, dt, J = 3.6, 9.1 Hz), 4.01 (1H, dd, J = 3.0, 11.6 Hz), 3.75 (1H, dd, J = 3.6, 11.6 Hz), 3.30 (1H, dd, J = 6.7, 14.4 Hz), 2.89 (1H, dd, J = 6.1, 14.4 Hz), 2.01 (3H, s), 1.94 (3H, s), 1.01 (9H, s). ^{13}C NMR

(125 MHz, $CDCl_3$): 169.8, 164.0, 154.9, 140.1, 135.7, 135.6, 133.8, 133.2, 133.0, 130.5, 129.7, 129.5, 128.8, 128.6, 128.4, 127.7, 127.6, 125.6, 107.7, 92.7, 91.7, 86.6, 80.3, 72.9, 62.9, 48.5, 26.8, 20.7, 19.2, 7.4. FTIR (neat): 1746, 1600 cm^{-1}. HRMS (ESI) *m/z*: calcd for $C_{42}H_{45}N_2O_7Si$ $(M+H)^+$ 717.2991, found 717.3032.

4.2.5. (1′*S*,3′*R*,4′*R*,5′*R*,7′*R*)-*N*²-Benzoyl-1-{4′-acetoxy-1′-phenyl-3′-(*t*-butyldiphenylsilyloxymethyl)-2′,6′-dioxabicyclo[3.3.0]oct-7′-yl}-4-methyl-3-pyrazolin-5-one (8a)

(WNA-1αMP) ^1H NMR (400 MHz, $CDCl_3$): δ 8.19 (2H, dd, J = 1.2, 7.9 Hz), 7.67–7.21 (19H, m), 6.17 (1H, t, J = 6.5 Hz), 4.98 (1H, dd, J = 4.5, 9.1 Hz), 4.71 (1H, d, J = 4.2 Hz), 4.21 (1H, d, J = 9.1 Hz), 4.00 (1H, dd, J = 2.4, 11.8 Hz), 3.65 (1H, dd, J = 5.5 Hz, 14.9 Hz), 3.59 (1H, dd, J = 2.4, 11.8 Hz), 2.88 (1H, dd, J = 7.9, 14.9 Hz), 1.92 (3H, s), 1.90 (3H, s), 0.97 (9H, s). FTIR (neat): 1750, 1600, 1239 cm^{-1}. HRMS (ESI) *m/z*: calcd for $C_{42}H_{45}N_2O_7Si$ $(M+H)^+$ 717.2991, found 717.3028.

4.2.6. (1′*S*,3′*R*,4′*R*,5′*R*,7′*S*)-*N*²-Benzoyl-1-{4′-acetoxy-1′-phenyl-3′-(*t*-butyldiphenylsilyloxymethyl)-2′,6′-dioxabicyclo[3.3.0]oct-7′-yl}-4-methyl-3-pyrazolin-5-one (8b)

(WNA-1βMP) ^1H NMR (400 MHz, $CDCl_3$): δ 8.21 (2H, dd, J = 1.2, 7.9 Hz), 7.70–7.21 (19H, m), 6.14 (1H, t, J = 6.7 Hz), 5.04 (1H, dd, J = 3.6, 9.2 Hz), 4.98 (1H, d, J = 3.9 Hz), 4.20 (1H, dt, J = 3.3, 9.4 Hz), 3.93 (1H, dd, J = 3.0, 11.6 Hz), 3.68 (1H, dd, J = 3.6, 11.6 Hz), 3.39 (1H, dd, J = 7.0, 14.3 Hz), 2.87 (1H, dd, J = 6.7, 14.3 Hz), 1.92 (3H, s), 1.90 (3H, s), 0.97 (9H, s). FTIR (neat): 1751, 1600, 1240 cm^{-1}. HRMS (ESI) *m/z*: calcd for $C_{42}H_{45}N_2O_7Si$ $(M+H)^+$ 717.2991, found 717.2979.

4.3. General procedure for deprotection reaction

A THF solution of the above compound and TBAF (1.0 M THF solution, 2 equiv) was stirred for 3.5 h at room temperature. MeOH and a 0.2 M aqueous NaOH solution (2 equiv) were then added to this mixture at 0 °C. After stirring for 2.5 h at 0 °C, the reaction was quenched with acetic acid and diluted with MeOH. The solvents were removed under reduced pressure. The residue was purified by flash silica gel column chromatography ($CHCl_3$/CH_3OH = 10:1) to give the corresponding diol compound.

4.3.1. (1′*S*,3′*R*,4′*R*,5′*R*,7′*R*)-*N*³-Dimethylaminomethylidine-1-(4′-hydroxy-3′-hydroxymethyl-1′-phenyl-2′,6′-dioxabicyclo[3.3.0]oct-7′-yl)-3-aminopyrazole (4a)

(WNA-αAP) ^1H NMR (400 MHz, $CDCl_3$): δ 7.73 (1H, s), 7.50 (2H, d, J = 7.3 Hz), 7.44 (1H, s), 7.38 (2H, t, J = 7.6 Hz), 7.28 (1H, t, J = 7.3 Hz), 6.63 (1H, t, J = 7.1 Hz), 5.71 (1H, s), 4.53 (1H, d, J = 6.7 Hz), 4.34–4.32 (1H, m), 4.04 (1H, d, J = 7.3 Hz), 4.00 (1H, dd, J = 1.8, 10.8 Hz), 3.80 (1H, dd, J = 4.6, 10.8 Hz), 3.23 (1H, dd, J = 6.7, 14.6 Hz), 3.03 (6H, s), 2.79 (1H, dd, J = 7.3, 14.6 Hz). ^{13}C NMR (125 MHz, $CDCl_3$): 154.9, 151.7, 144.0, 140.1, 128.6, 127.4, 127.6, 124.3, 92.6, 89.9, 87.9, 86.8, 83.2, 72.1, 62.7, 46.0, 40.4, 34.6. FTIR (neat): 3351, 1633 cm^{-1}. HRMS (ESI) *m/z*: calcd for $C_{19}H_{25}N_4O_4$ $(M+H)^+$ 373.1870, found 373.1908.

4.3.2. (1′*S*,3′*R*,4′*R*,5′*R*,7′*S*)-*N*³-Dimethylaminomethylidine-1-(4′-hydroxy-3′-hydroxymethyl-1′-phenyl-2′,6′-dioxabicyclo[3.3.0]-oct-7′-yl)-3-aminopyrazole (4b)

(WNA-βAP) ^1H NMR (400 MHz, $CDCl_3$): δ 7.75 (1H, s), 7.65 (2H, d, J = 7.6 Hz), 7.46 (1H, s), 7.36 (2H, t, J = 7.6 Hz), 7.26 (1H, t, J = 7.3 Hz), 6.66 (1H, t, J = 7.0 Hz), 5.73 (1H, s), 4.86 (1H, d, J = 3.6 Hz), 4.07 (1H, d, J = 2.4 Hz), 4.01 (1H, d, J = 3.9 Hz), 3.99 (1H, dd, J = 3.3, 12.0 Hz), 3.80 (1H, dd, J = 4.9, 12.0 Hz), 3.45 (1H, dd, J = 7.9, 13.9 Hz), 3.06 (6H, s), 2.82 (1H, dd, J = 6.1, 13.9 Hz). ^{13}C NMR (125 MHz, $CDCl_3$): 154.9, 151.9, 140.8, 140.3, 128.5, 127.6, 125.3, 92.4, 89.9, 87.9, 85.5, 84.0, 73.1, 63.2, 47.5, 40.4, 34.6. FTIR (neat): 3368, 1633 cm^{-1}. HRMS (ESI) *m/z*: calcd for $C_{19}H_{25}N_4O_4$ $(M+H)^+$ 373.1870, found 373.1898.

4.3.3. (1′*S*,3′*R*,4′*R*,5′*R*,7′*R*)-2-(4′-Hydroxy-3′-hydroxymethyl-1′-phenyl-2′,6′-dioxabicyclo[3.3.0]oct-7′-yl)-4-methyl-3-pyrazolin-5-one (9a)

(WNA-2αMP) ^1H NMR (400 MHz, CD_3OD): δ 7.60 (2H, d, J = 8.2 Hz), 7.47 (1H, s), 7.37 (2H, t, J = 7.3 Hz), 7.27 (1H, t, J = 7.3 Hz), 6.38 (1H, t, J = 6.6 Hz), 4.45 (1H, d, J = 4.3 Hz), 4.15–4.12 (1H, m), 3.87–3.84 (2H, m), 3.69 (1H, dd, J = 6.4, 11.9 Hz), 2.87 (1H, d, J = 6.6 Hz), 1.86 (3H, s). ^{13}C NMR (125 MHz, CD_3OD): 162.5, 143.6, 131.0, 129.4, 128.5, 126.2, 103.6, 93.0, 90.5, 83.2, 73.1, 63.4, 48.3, 7.0. FTIR (neat): 3354, 1708, 1603, 1528 cm^{-1}. HRMS (ESI) *m/z*: calcd for $C_{17}H_{21}N_2O_5$ $(M+H)^+$ 333.1445, found 333.1473.

4.3.4. (1′*S*,3′*R*,4′*R*,5′*R*,7′*S*)-2-(4′-Hydroxy-3′-hydroxymethyl-1′-phenyl-2′,6′-dioxabicyclo[3.3.0]oct-7′-yl)-4-methyl-3-pyrazolin-5-one (9b)

(WNA-2βMP) ^1H NMR (400 MHz, CD_3OD): δ 7.73 (2H, d, J = 7.6 Hz), 7.38 (1H, s), 7.34 (2H, t, J = 7.3 Hz), 7.24 (1H, t, J = 7.3 Hz), 6.00 (1H, t, J = 6.8 Hz), 4.66 (1H, d, J = 3.6 Hz), 4.05–4.00 (1H, m), 3.88 (1H, dd, J = 2.1, 11.9 Hz), 3.81 (1H, dd, J = 3.6, 10.7 Hz), 3.68 (1H, dd, J = 6.1, 10.7 Hz), 3.12 (1H, dd, J = 7.9, 14.0 Hz), 2.69 (1H, dd, J = 6.1, 14.0 Hz), 1.92 (3H, s). ^{13}C NMR (125 MHz, CD_3OD): 162.7, 142.5, 131.9, 129.3, 128.4, 126.6, 102.9, 93.2, 90.0, 84.5, 73.6, 63.7, 49.1, 6.9. FTIR (neat): 3386, 1609, 1530 cm^{-1}. HRMS (ESI) *m/z*: calcd for $C_{17}H_{21}N_2O_5$ $(M+H)^+$ 333.1445, found 333.1420.

4.4. General procedure of synthesis for the WNA-AP phosphoramidite

DMTrCl (3 equiv) was added to a solution of the diol compound in pyridine. After stirring for 1 h, the reaction mixture was diluted with EtOAc, and then washed with water and brine. The organic layer was washed with water and brine, dried over Na_2SO_4, evaporated, and then the residue was purified by flash silica gel column chromatography ($CHCl_3$/CH_3OH = 99:1 containing 0.5% pyridine) to give the corresponding DMTr-protected WNA. iP_2NEt (6 equiv) was added to a solution of the above DMTr-WNA and $iPr_2NP(Cl)OC_2H_4CN$ (3 equiv) in CH_2Cl_2 at 0 °C. After stirring for 1 h, the reaction mixture was diluted with an aqueous saturated $NaHCO_3$ solution, and extracted with EtOAc. The organic layer was dried over Na_2SO_4, evaporated, then the residue was purified by flash silica gel column chromatography (hexane/EtOAc = 1:1) to give the purified materials.

4.4.1. (1′*S*,3′*R*,4′*R*,5′*R*,7′*R*)-*N*³-Dimethylaminomethylidine-1-{3′-dimethoxytrithyloxymethyl-4′-*O*-(*N*,*N*-diisopropyl-β-cyanoethylphosphoramidyl)-1′-phenyl-2′,6′-dioxabicyclo[3.3.0]oct-7′-yl}-3-aminopyrazole (5a)

(WNA-αAP) ^1H NMR (400 MHz, $CDCl_3$): δ 7.74 (1H, s), 7.67 (1H, d, J = 7.3 Hz), 7.50–7.15 (12H, m), 6.78 (4H, dd, J = 1.5, 8.8 Hz), 6.60 (1H, t, J = 7.0 Hz), 5.67 (1H, s), 4.69–4.65 (1H, m), 4.50 (1H, d, J = 4.8 Hz), 4.38–4.37 (1H, m), 3.99–3.87 (1H, m), 3.76 (6H, s), 3.77 (6H, s), 3.76–3.17 (7H, m), 3.05–3.01 (6H, m), 2.88–2.82 (1H, m), 1.06–0.78 (9H, m). ^{31}P NMR (162 MHz, $CDCl_3$): 149.32, 146.96. FTIR (neat): 2836, 1635, 1508, 1251 cm^{-1}. ESI-MS (*m/z*) 876.56 $[M+H]^+$.

4.4.2. (1′*S*,3′*R*,4′*R*,5′*R*,7′*S*)-*N*³-Dimethylaminomethylidine-1-{3′-dimethoxytrithyloxymethyl-4′-*O*-(*N*,*N*-diisopropyl-β-cyanoethylphosphoramidyl)-1′-phenyl-2′,6′-dioxabicyclo[3.3.0]oct-7′-yl}-3-aminopyrazole (5b)

(WNA-βAP) ^1H NMR (400 MHz, $CDCl_3$): δ 7.89 (1H, d, J = 7.0 Hz), 7.82 (1H, d, J = 7.0 Hz), 7.75 (0.5H, s), 7.68 (0.5H, s), 7.50–7.44

(2.5H, m), 7.41–7.34 (4.5H, m), 7.29–7.17 (4H, m), 6.79 (4H, d, J = 8.8 Hz), 6.73–6.69 (1H, m), 5.69 (0.5H, d, J = 1.8 Hz), 5.64 (0.5H, d, J = 2.1 Hz), 4.85 (1H, dd, J = 3.6, 14.0 Hz), 4.38–4.37 (1H, m), 4.24–4.18 (0.5H, m), 4.00–3.95 (0.5H, m), 3.77 (6H, s), 3.74–3.68 (0.5H, m), 3.50–3.20 (6H, m), 3.02 (6H, s), 2.97–2.90 (1H, m), 2.56–2.48 (0.5H, m), 2.36–2.25 (1.5H, m), 2.14 (0.5H, s), 1.05–1.00 (6H, m), 0.88–0.84 (6H, m), 0.78 (2H, d, J = 6.7 Hz). ^{31}P NMR (162 MHz, $CDCl_3$): 149.13, 148.41. FTIR (neat): 2836, 1635, 1508, 1250 cm^{-1}. ESI-MS (m/z) 876.56 [M+H]$^+$.

4.5. General procedure of synthesis for WNA-MP phosphoramidite

DMTrCl (3 equiv) was added to a solution of the diol compound in pyridine. After stirring for 1 h, the reaction mixture was diluted with EtOAc, and then washed with water and brine. The organic layer was washed with water and brine, dried over Na_2SO_4, evaporated, and then the residue was purified by flash silica gel column chromatography ($CHCl_3$/CH_3OH = 99:1 containing 0.5% pyridine) to give the corresponding DMTr-protected WNA. Acetic anhydride (1.2 equiv) was added to the solution of DMTr-WNA in pyridine. After stirring for 2 h, the reaction mixture was diluted with EtOAc and washed with an aqueous saturated NaCl solution. The organic layer was dried over Na_2SO_4, evaporated, then the residue was purified by flash silica gel column chromatography ($CHCl_3$/CH_3OH = 99:1 containing 0.5% pyridine) to give the purified DMTr-Ac-protected WNA. iP$_2$NEt (6 equiv) was added to a solution of the above DMTr-Ac-WNA and (iPr$_2$N)$_2$POC$_2$H$_4$CN (3 equiv) in CH_2Cl_2 at 0 °C. After stirring for 1 h, the reaction mixture was diluted with a satd $NaHCO_3$ solution, and extracted with EtOAc. The organic layer was dried over Na_2SO_4, and evaporated, and then the residue was purified by flash silica gel column chromatography (hexane/EtOAc = 1:1) to give the purified materials.

4.5.1. (1′*S*,3′*R*,4′*R*,5′*R*,7′*R*)-*N*^{1}-Acethyl-2-{3′-dimethoxytrithyloxymethyl-4′-*O*-(*N*,*N*-diisopropyl-β-cyanoethylphosphoramidyl)-1′-phenyl-2′,6′-dioxabicyclo[3.3.0]oct-7′-yl}-4-methyl-3-pyrazolin-5-one (11a)

(WNA-2αMP) ^{1}H NMR (400 MHz, $CDCl_3$): δ 7.75 (0.3H, s), 7.72 (0.7H, s), 7.57 (1.4H, d, J = 7.0 Hz), 7.55 (0.6H, d, J = 7.0 Hz), 7.42 (2H, d, J = 7.0 Hz), 7.34–7.16 (10H, m), 6.78 (4H, d, J = 8.8 Hz), 6.20–6.15 (1H, m), 4.72 (0.3H, d, J = 3.9 Hz), 4.62 (0.7H, d, J = 3.9 Hz), 4.28 (0.7H, t, J = 3.9, 9.3 Hz), 4.18–4.16 (0.3H, m), 4.09 (0.7H, m), 3.96–3.95 (0.3H, m), 3.77 (6H, s), 3.73–3.70 (1H, m), 3.55–3.46 (2H, m), 3.44–3.38 (2H, m), 2.34–3.15 (2H, m), 2.96–2.89 (1H, m), 2.29 (0.9H, s), 2.28 (2.1H, s), 1.95 (0.9H, s), 1.92 (2.1H, s), 1.33–1.18 (3H, m), 1.09 (4H, d, J = 6.7 Hz), 1.04 (1.8H, d, J = 6.7 Hz), 1.03 (4.2H, d, J = 6.7 Hz), 0.83 (2H, d, J = 6.7 Hz). ^{31}P NMR (162 MHz, $CDCl_3$): 150.21, 148.85. FTIR (neat): 2252, 1766, 1607, 1583, 1508 cm^{-1}. ESI-MS (m/z) 878.43 [M+H]$^+$.

4.5.2. (1′*S*,3′*R*,4′*R*,5′*R*,7′*S*)-*N*^{1}-Acethyl-2-{3′-dimethoxytrithyloxymethyl-4′-*O*-(*N*,*N*-diisopropyl-β-cyanoethylphosphoramidyl)-1′-phenyl-2′,6′-dioxabicyclo[3.3.0]oct-7′-yl}-4-methyl-3-pyrazolin-5-one (11b)

(WNA-2βMP) ^{1}H NMR (400 MHz, $CDCl_3$): δ 7.65 (2H, d, J = 6.7 Hz), 7.45 (2H, t, J = 7.6 Hz), 7.38–7.18 (11H, m), 6.79 (4H, d, J = 8.8 Hz), 6.12–6.06 (1H, m), 4.79 (0.5H, d, J = 3.6 Hz), 4.71 (0.5H, d, J = 2.7 Hz), 4.33–4.22 (1.5H, m), 4.03–3.98 (0.5H, m), 3.78 (3H, s), 3.77 (3H, s), 3.72 (1H, dd, J = 6.7, 14.8 Hz), 3.50–3.19 (6H, m), 3.00–2.92 (1H, m), 2.47 (1H, t, J = 6.4 Hz), 2.32 (2H, s), 2.31 (2H, s), 1.91 (1.5H, s), 1.89 (1.5H, s), 1.07 (3H, d, J = 6.7 Hz), 1.04 (3H, d, J = 6.7 Hz), 0.95 (3H, d, J = 6.7 Hz), 0.82 (3H, d, J = 6.7 Hz). ^{31}P NMR (162 MHz, $CDCl_3$): 150.52, 149.27. FTIR (neat): 2252, 1766, 1607, 1583, 1508 cm^{-1}. ESI-MS (m/z) 878.66 [M+H]$^+$.

4.6. Synthesis of triplex-forming oligonucleotides

The triplex-forming oligonucleotides (TFOs) containing WNA analogs having the pyrazole ring as a recognition base were synthesized using an automated DNA synthesizer (Applied Biosystems 394 DNA/RNA Synthesizer). After cleavage from CPG, they were purified by HPLC (HPLC conditions: COSMOSIL 5C18-MS-II (10 × 250 mm), Buffer; A: 0.1 M TEAA, B: CH_3CN, 10–40%/20 min, 40–100%/30 min linear gradient, Flow rate; 3.0 mL/min, UV-detector; 254 nm). All the synthesized TFOs were identified by the MALDI-TOF MS (negative mode) measurements. MALDI-TOF MASS results: **TFO1(βAP)**: calcd for 5815.05, found 5814.78, **TFO1(αAP)**: calcd for 5815.05, found 5811.49, **TFO1(2βMP)**: calcd for 5830.27, found 5832.73, **TFO1(2αMP)**: calcd for 5830.27 found 5829.18, **TFO2(βAP)**: calcd for 5831.04, found 5831.01, **TFO2(αAP)**: calcd for 5831.04, found 5831.38, **TFO2(2βMP)**: calcd for 5846.26, found 5846.64, **TFO2(2αMP)**: calcd for 5846.26 found 5846.49, **TFO3(βAP)**: calcd for 5815.05, found 5814.04, **TFO3(αAP)**: calcd for 5810.05, found 5810.33, **TFO3(2βMP)**: calcd for 5830.27, found 5828.69, **TFO3(2αMP)**: calcd for 5830.27 found 5829.46, **TFO4(βAP)**: calcd for 5799.06, found 5799.73, **TFO4(αAP)**: calcd for 5799.06, found 5797.73, **TFO4(2βMP)**: calcd for 5814.28, found 5810.75, **TFO4(2αMP)**: calcd for 5814.28 found 5812.68.

4.7. Evaluation of triplex formation by the gel-shift assay

The triplex formation was performed for 12 h at 22 °C in a buffer containing 20 mM Tris–HCl, 5 mM $MgCl_2$, 2.5 mM spermidine and 10% sucrose at pH 7.5, and analyzed by electrophoresis at 10 °C with a 20% non-denatured polyacrylamide gel. Ten nM TFO containing the ^{32}P-labeled one as the tracers was used. The TFO and the triplex bands were quantified to produce the relative concentrations, and the association constant was calculated using the concentration of each component and the following equation, K_s = [Triplex]/[Duplex][TFO].

Acknowledgments

S.S. and Y.T. are grateful for the support by a Grant-in-Aid for Scientific Research (A) and Young Scientists (B) from the Japan Society for the Promotion of Science (JSPS), and CREST from the Japan Science and Technology Agency.

References and notes

1. Duca, M.; Vekhoff, P.; Oussedik, K.; Halby, L.; Arimondo, P. B. *Nucleic Acids Res.* **2008**, *36*, 5123.
2. Rusling, D. A.; Broughton-Head, V. J.; Brown, T.; Fox, K. R. *Curr. Chem. Biol.* **2008**, *2*, 1.
3. Simon, P.; Cannata, F.; Concordet, J.-P.; Giovannangeli, C. *Biochimie* **2008**, *90*, 1109.
4. Lange, S. S.; Reddy, M. C.; Vasquez, K. M. *DNA Repair* **2009**, *8*, 865.
5. Chin, J. Y.; Glazer, P. M. *Mol. Carcinog.* **2009**, *48*, 389.
6. Benfield, A. P.; Macleod, M. C.; Lie, Y.; Wu, Q.; Wensel, T. G.; Vasquez, K. M. *Biochemistry* **2008**, *47*, 6279.
7. Ghosh, M. K.; Katyal, A.; Chandra, R.; Brahmachari, V. *Mol. Cell. Biochem.* **2005**, *278*, 147.
8. Soyfer, V. N.; Potaman, V. N. *Triple-Helical Nucleic Acids*; Springer: New York, 1996.
9. Parel, S. P.; Leumann, C. J. *Nucleic Acids Res.* **2001**, *29*, 2260.
10. Obika, S.; Inohara, H.; Hari, Y.; Imanishi, T. *Bioorg. Med. Chem.* **2008**, *16*, 2945.
11. Obika, S.; Hari, Y.; Sekiguchi, M.; Imanishi, T. *Chem. Eur. J.* **2002**, *8*, 4796.
12. Guianvarc'h, D.; Fourrey, J.-L.; Maurisse, R.; Sun, J.-S.; Benhida, R. *Bioorg. Med. Chem.* **2003**, *11*, 2751.
13. Rusling, D. A.; Peng, G.; Srinivasan, N.; Fox, K. R.; Brown, T. *Nucleic Acids Res.* **2009**, *37*, 1288.
14. Sasaki, S.; Yamauchi, H.; Nagatsugi, F.; Takahashi, R.; Taniguchi, Y.; Maeda, M. *Tetrahedron Lett.* **2001**, *42*, 6915.
15. Sasaki, S.; Taniguchi, Y.; Takahashi, R.; Senko, Y.; Kodama, K.; Nagatsugi, F.; Maeda, M. *J. Am. Chem. Soc.* **2004**, *126*, 516.
16. Taniguchi, Y.; Sasaki, S. *J. Synth. Org. Chem., Jpn.* **2004**, *62*, 1026.

17. Taniguchi, Y.; Nakamura, A.; Senko, Y.; Kodama, K.; Nagatsugi, F.; Sasaki, S. *Nucleosides Nucleotides Nucleic Acids* **2005**, *24*, 823–827.
18. Taniguchi, Y.; Nakamura, A.; Senko, Y.; Nagatsugi, F.; Sasaki, S. *J. Org. Chem.* **2006**, *71*, 2115.
19. Taniguchi, Y.; Togo, M.; Aoki, E.; Uchida, Y.; Sasaki, S. *Tetrahedron* **2008**, *64*, 7164.
20. Maquesriau, A.; Eynde, J.-J. V. *Tetrahedron* **1987**, *43*, 4185.
21. Sommer, T. J. *Synthesis* **2004**, 161.